



Wireless and real-time structural damage detection: A novel decentralized method for wireless sensor networks

Onur Avci ^{a,*}, Osama Abdeljaber ^a, Serkan Kiranyaz ^b, Mohammed Hussein ^a, Daniel J. Inman ^c

^a Department of Civil Engineering, Qatar University, Qatar

^b Department of Electrical Engineering, Qatar University, Qatar

^c Department of Aerospace Engineering, University of Michigan, Ann Arbor, MI, USA

ARTICLE INFO

Article history:

Received 24 September 2017

Received in revised form 7 March 2018

Accepted 11 March 2018

Available online 21 March 2018

Keywords:

Structural damage detection
Convolutional neural networks
Infrastructure health
Structural health monitoring
Wireless sensor networks
Real-time damage detection

ABSTRACT

Being an alternative to conventional wired sensors, wireless sensor networks (WSNs) are extensively used in Structural Health Monitoring (SHM) applications. Most of the Structural Damage Detection (SDD) approaches available in the SHM literature are *centralized* as they require transferring data from all sensors within the network to a single processing unit to evaluate the structural condition. These methods are found predominantly feasible for wired SHM systems; however, transmission and synchronization of huge data sets in WSNs has been found to be arduous. As such, the application of centralized methods with WSNs has been a challenge for engineers. In this paper, the authors are presenting a novel application of 1D Convolutional Neural Networks (1D CNNs) on WSNs for SDD purposes. The SDD is successfully performed completely wireless and real-time under ambient conditions. As a result of this, a *decentralized* damage detection method suitable for wireless SHM systems is proposed. The proposed method is based on 1D CNNs and it involves training an individual 1D CNN for each wireless sensor in the network in a format where each CNN is assigned to process the locally-available data only, eliminating the need for data transmission and synchronization. The proposed damage detection method operates directly on the raw ambient vibration condition signals without any filtering or preprocessing. Moreover, the proposed approach requires minimal computational time and power since 1D CNNs merge both feature extraction and classification tasks into a single learning block. This ability is prevailingly cost-effective and evidently practical in WSNs considering the hardware systems have been occasionally reported to suffer from limited power supply in these networks. To display the capability and verify the success of the proposed method, large-scale experiments conducted on a laboratory structure equipped with a state-of-the-art WSN are reported.

© 2018 Elsevier Ltd. All rights reserved.

* Corresponding author.

E-mail addresses: onur.avci@qu.edu.qa (O. Avci), o.abdeljaber@qu.edu.qa (O. Abdeljaber), mkiranyaz@qu.edu.qa (S. Kiranyaz), mhussein@qu.edu.qa (M. Hussein), daninman@umich.edu (D.J. Inman).

1. Introduction

Aging of civil infrastructure is inevitable as they are widely exposed to short term and long term damage during their life-cycle [1,2]. While the inspection of civil engineering infrastructure has generally been difficult and costly due to their large size compared to other engineering structures, the traditional structural damage detection (SDD) methods of civil infrastructure rely heavily on frequent visual inspection [3–5]. However, visual inspection is not economical particularly when the targeted structural members are difficult to reach and/or blocked with other structural and/or non-structural elements [6,7]. The visual inspections have evolved into “monitoring” in time and researchers have been continually working on developing more feasible SDD methods in the area of structural health monitoring (SHM) ever since [8].

Sensor units are imperative for monitoring the health of civil infrastructure [9–11]. Traditionally, wired sensors have been used in SHM applications due to their availability in the market before the wireless ones [12,13]. The use of wired sensors for SHM of large structures was found challenging due to various hardships in installation and maintenance of the wiring system [14]. Following the advancements in the sensor technology, wireless sensor networks (WSNs) have been progressively utilized in SHM and SDD [15–24]. However, there are some challenges regarding the use of WSNs in SDD [25–27]. Most of the damage detection approaches available in the literature are centralized as they require transferring data from all sensors within the network to a single processing unit in order to evaluate the structural condition [28,29]. Such methods are indeed feasible for wired SHM systems [30]; however, transmission and synchronization of huge amounts of data in WSNs have been reported to be problematic. Therefore, the application of centralized methods with WSNs can be burdensome [31]. Another challenge is that wireless sensor units usually have limited power supplies [32].

A big portion of the vibration-based SDD methods available in the literature require a three-step process: data pre-processing, feature extraction, and feature classification [33]. The feature extraction is simply extracting damage-sensitive features from the preprocessed vibrations [34]. Feature classification stage involves utilizing a certain classifier to classify the extracted feature in order to figure out whether they belong to the undamaged or damaged state [35,36]. Such process requires significant computational power which is usually not readily available in wireless sensing units.

The goal of this paper is to overcome the aforementioned challenges by developing and testing a decentralized and computationally-inexpensive damage detection method based on 1D convolutional neural networks (1D CNNs). For that purpose, in this paper, the authors are proposing to use 1D CNNs on WSNs. The SDD is successfully performed completely wireless and real-time, under ambient vibration conditions. As a result of this, a decentralized damage detection method suitable for wireless SHM systems is proposed. The proposed system is tested on a large-scale laboratory structure equipped with state-of-the-art wireless sensing units. The work presented in this paper can be considered as a significant upgrade and improvement on the previous work by the authors [33,37] in which the 1D CNNs were utilized on a wired accelerometer system, under shaker excitations.

The proposed SDD system involves training of an individual CNN for each wireless unit in the WSN. In this system, each CNN is responsible for processing the locally-available data only, in a decentralized manner. This feature eliminates the need for transmitting and synchronizing the data at a central processing unit. The most compelling feature of 1D CNNs is their ability to merge both feature extraction and feature classification stages into a single block which significantly reduces the required computational time and effort. The damage detection method proposed in this paper runs immediately on the raw ambient vibration condition signals without any filtering or preprocessing. In addition, the proposed damage detection system utilizes a network of triaxial wireless units. As explained later in the paper, the CNN training process takes into account the ambient vibration signals measured along the three directions at each node of the WSN. This is done to figure out the direction along which the damage features are more pronounced.

The paper is organized in a way that a brief review of the recent applications of WSNs and CNNs are presented in Sections 2 and 3, respectively. Laboratory test setup and instrumentation are explained in Section 4. Overview, adaptation, and the back-propagation training of 1D CNNs are presented in Section 5. The proposed wireless and real-time 1D CNN-based damage detection algorithm is explained in Section 6. The experiments conducted to demonstrate the algorithm using Qatar University Grandstand Simulator (QUGS) along with the results and performance evaluation are displayed in Section 7. The conclusions are listed in Section 8.

2. Wireless sensor network use in structural health monitoring applications

It did not take long time for the SHM researchers to observe the fact that, when used in an array format, the wireless sensors can work in a network system through which the SHM processes can be run in a more practical, economical and advanced way [38,39]. The most obvious advantages of WSNs recognized in the beginning were avoiding kilometers of cable work, installation costs and associated expenses but many other advantages were identified later [40]. Yet, the WSNs had their own challenges (e.g. transmission, synchronization, limited communications bandwidth, adaptability, limited energy supply, limited memory and computational capability and etc.) on which countless studies such as mobile agent approach [41], active sensing platforms [42], smart sensors [43], reconfigurable sensors [44], eigen-system realization algorithms [45], two-tiered approaches [46], capacitance-based and impedance-based wireless sensors [47], enhanced damage locating vectors [48], zigbee technology [49], embedded goertzel algorithm [50], compressive sampling–based data loss recovery [51], operating with limited sensors [48] and many other notable work were performed to contribute to and enhance the SHM processes.

In addition, the wireless SHM work on ultrasonic guided waveform response [52], information-fusing firefly algorithm [53], fault diagnosis [54], cluster-based optimal deployment [55], dependable distribution framework [56], low-rank and sparse data [57] are some of the most recent work setting the trend in SHM with WSNs.

The SDD approaches are predominantly centralized as they require transferring data from all sensors within the network to a single processing unit in order to assess the structural integrity. These approaches are applicable and relatively economical for wired sensor systems; whereas for wireless systems, the transmission, synchronization and aggradation of large data have become often pronounced difficulties. Computing and power limitations; and security and reliability concerns are additional hindrance associated with centralized methods [31]. All this brings the need for a decentralized damage detection method. The method would reduce the latency and energy consumption for the sensors and would be more suitable for wireless SHM systems [58]. Such method is developed, proposed and verified in this paper. The proposed decentralized damage detection method is based on 1D CNNs and it eliminates the need for data transmission and synchronization; requiring only minimal computational time and power.

3. Most recent 1D and 2D convolutional neural network applications

As mentioned earlier, the objective of this study is to overcome the challenges associated with the use of WSNs in SDD by using CNNs. CNNs have been widely accepted as a standard for “Deep Learning” methods since they revealed excellent performance [59–61]. CNNs are predominantly feed-forward artificial neural networks (ANNs) housing alternating sub-sampling and convolutional layers. The convolutional layers simply represent the cells of human visual cortex [62], CNNs are developed primarily for 2D signals (e.g. video frames and images). Nevertheless, 1D CNNs have been successfully utilized for the classification of electrocardiogram (ECG) beats [63,64] revealing excellent performance in both speed and accuracy. In addition, most recently, 1D CNNs have been successfully utilized for fault detection in high power engines [65], fault detection for rotating machinery [66], bearing fault diagnosis [67], and fault detection of planetary gearbox [68]. The success of the CNNs is due to the fact that linear filters are utilized by convolutional layers and filter parameters are *optimized* during the training process. The linear filters extract such features that can characterize the object/pattern in an image/signal. The convolutional layers are followed by a feed-forward and fully connected layers, which are the same as the hidden layers of Multi-layer Perceptrons (MLPs) where the classification task is mainly realized. As such, independent of the variations in the signal characteristics and patterns, CNNs have the natural ability to learn the optimal features and the classifier parameters in a combined optimization process, the so-called Back-Propagation.

Application of the 1D CNNs is relatively new in vibration based SDD. Recently, the authors have developed a SDD algorithm using 1D CNNs [33,37]. This algorithm was used to monitor a laboratory structure instrumented with uniaxial wired accelerometers. To the best information of the authors, the laboratory structure is the largest stadium structure in the world, built in a laboratory environment [69]. The 1D CNNs were trained and used to process the vibration response of the structure under shaker excitations in order to obtain specific damage indices that reflect the condition of the structure. The algorithm is proved to be a successful and efficient vibration-based SDD tool to sense and localize structural damage. It should be emphasized that the algorithm was also tested and validated to be a successful on a benchmark data, collected by others [70].

In the study presented herein, the algorithm used in Refs. [33,37] is further improved in order to address the following issues:

1. The algorithm proposed in Refs. [33,37] requires obtaining the response of the monitored structure under external excitation generated by an electrodynamic shaker. While this approach is applicable for small structures in a laboratory environment, it is quite difficult to apply it for extremely heavy real-life civil structures. Therefore, in this paper, the CNNs are trained using only the raw vibration signals measured under ambient conditions.
2. In Refs. [33,37], uniaxial wired accelerometers were utilized to measure the vibration response at each joint along the vertical direction only. This allowed for analyzing the effect of structural damage along just a single direction. To address this issue, the study presented in this paper utilizes state-of-the-art triaxial wireless sensing units to measure the ambient vibration response along the three directions at each location. Therefore, the CNN-based algorithm is modified so that it can analyze the three signals at each node in order find out the direction along which the damage features are more distinguishable, and therefore, enhance the classification performance.

4. Laboratory test setup and instrumentation

The newly developed methods like the one proposed in this paper should be experimentally verified in a laboratory environment before they can be applied to real structures, outside the laboratory. It is important for the test structure to be large enough to simulate the similar conditions of a real structure, or a portion of a real structure.

The Qatar University Grandstand Simulator (QUGS) is utilized for the experimental testing for the work presented in this paper. QUGS is the largest stadium structure in the world, built in a laboratory environment. Having projected plan dimensions of $4.2 \text{ m} \times 4.2 \text{ m}$, the steel structure is capable of hosting thirty spectators at a time. The QUGS is a test bed for vibrations serviceability, SDD and SHM research at Qatar University [69]. The main frame of QUGS consists of eight main

girders and twenty-five filler beams carried by four columns, as shown in Fig. 1. The main girders are 4.6 m long; the filler beams are 1 m in length at the cantilever portion and 77 cm everywhere else. Filler beams of the test structure are designed in a way that they are removable and interchangeable so that various structural damage scenarios are generated. For instance, the bolts can be loosened at filler beam connections; or any kind of flange damage and/or web damage can be introduced to the filler beams. In this perspective, the loosened bolts are a much lighter damage when compared to the physically damaged beams. This means it would be much more difficult to sense whether the bolts at a connection are loosened or not. As explained later in the paper, the proposed 1D CNN based algorithm is able to sense even slight damage of bolt loosening with wireless sensors in real-time, under ambient conditions.

The laboratory structure is instrumented with state-of-the-art wireless sensor network consisting of 10 TROMINO® ENGY units (Fig. 2). TROMINO units are triaxial sensors having 3 velocimetric and 3 accelerometric channels. These sensors are ultra-compact and relatively light weight which makes them ideal for stratigraphic applications, modal testing, and vibration serviceability assessment. One of the most interesting features of these sensors is the ability to synchronize multiple sensors by using either Radio synchronization or GPS time marker. The technical specifications of TROMINO sensors are summarized in Table 1. As shown in Figure, the sensors are located at the 10 beam-to-girder joints connecting the filler beams to the two horizontal girders illustrated in Fig. 3. The 10 sensors were firmly attached to the girder's flange by screws as shown in Fig. 4.

5. Synopsis of CNNs and back-propagation methodology for 1D CNNs

In machine learning, CNNs are a category of deep, biologically inspired feed-forward artificial neural networks which set a basic model for the visual cortex of mammals. Just like ordinary neural networks, CNNs consist of neurons that have learnable weights and biases; yet, they operate with the assumption that inputs are images, allowing the users to encode the properties as they like, as a result significantly reducing many parameters. CNNs have been effectively applied to several fields in object and event recognition systems. A 2D CNN model with an input layer for 28×28 pixel images is illustrated in Fig. 5.

Following the input layer, each convolution layer alternates with a sub-sampling layer. This layer decimates the propagated 2D maps from the neurons of the previous layer. As opposed to fixed and plain parameters of the 2D filter kernels, in CNNs they are trained and optimized by the back-propagation (BP) algorithm. Nevertheless, the sub-sampling factor and the kernel size, which are set to 2 and 5, respectively for presentation purposes in Fig. 5, are the two governing parameters of the CNN. While the input layer is a passive layer, it accepts an input image and assigns its color channels (Red, Green, Blue) as the feature maps of its three neurons. Being fully-connected and feed-forward, the following layers are the same as the hidden layers of a MLP. These so called fully-connected layers result in the output layer, producing the classification vector [33,65].

Since the learning stage is for SDD in this paper, an adaptive 1D CNN structure is utilized to blend extraction of features and “damage learning” stages of the raw accelerometer data of raw wireless sensors. In this process, the adaptive CNN topology will permit the variations in the input layer dimension. In addition to this, the compact CNN layer structure has now convolution layers' hidden neurons. The hidden neurons can run sub-sampling and convolution tasks as indicated in Fig. 6. Based on this, the merging of the sub-sampling and convolution layers are called as the “CNN layer” here in this paper in an attempt to show the distinction, yet continue to call the remaining layers as the fully-connected layers that are the same as the hidden layers of a MLP [33,65].

Other structural differences among the classical 2D and the proposed 1D CNNs can be summarized as the following. The significant difference is simply using 1D arrays for the place of 2D matrices for both kernels and feature maps. For 1D CNNs,

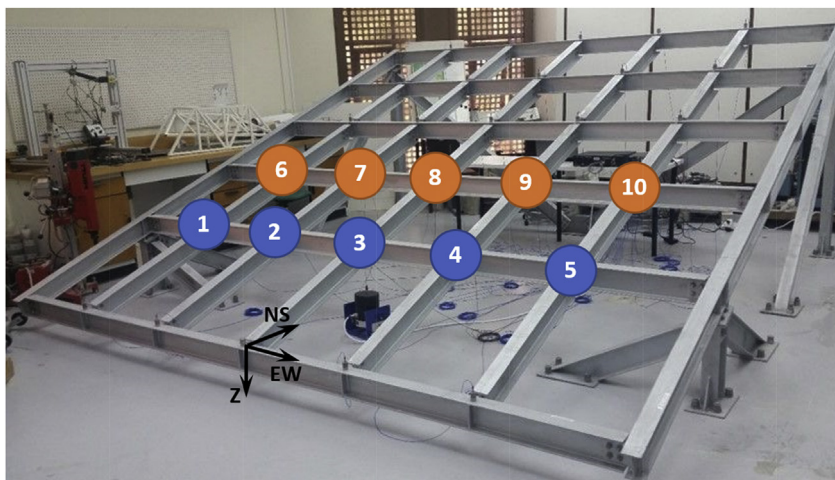


Fig. 1. Structural steel frame of the QUGS.



Fig. 2. TROMINO® ENGY wireless sensing unit.

the 2D matrix operations such as lateral rotation (*rot180*) and 2D convolution (*conv2D*) are replaced by *reverse* and *conv1D* operations [33,65].

In the CNN-layers, the one dimensional forward propagation (1D-FP) is defined by Equation (1):

$$\mathbf{x}_k^l = \mathbf{b}_k^l + \sum_{i=1}^{N_{l-1}} \text{conv1D}(\mathbf{w}_{ik}^{l-1}, \mathbf{s}_i^{l-1}) \quad (1)$$

where:

\mathbf{x}_k^l is defined as the input,

\mathbf{b}_k^l is defined as the bias of the k^{th} neuron at layer l

\mathbf{s}_i^{l-1} is defined as the output of the i^{th} neuron at layer $l-1$.

\mathbf{w}_{ik}^{l-1} is defined as the kernel from the i^{th} neuron at layer $l-1$ to the k^{th} neuron at layer l .

\mathbf{y}_k^l can be written from the input \mathbf{x}_k^l :

$$\mathbf{y}_k^l = f(\mathbf{x}_k^l) \quad \text{and} \quad \mathbf{s}_k^l = \mathbf{y}_k^l \downarrow ss \quad (2)$$

where \mathbf{s}_k^l stands for the output of the neuron and $\downarrow ss$ is for down-sampling operation with the factor, ss .

The back-propagation (BP) methodology is expressed as the following. The BP of the error starts from the output fully-connected layer. $l=1$ for the input layer and $l=L$ for the output layer. When N_L is the number of classes in the database; then, for an input vector \mathbf{p} , and its target and output vectors, \mathbf{t}_i^p and $[\mathbf{y}_1^l, \dots, \mathbf{y}_{N_L}^l]$. With that, in the output layer for the input \mathbf{p} ; E_p , the mean-squared error (MSE) is:

$$E_p = \text{MSE}(\mathbf{t}_i^p, [\mathbf{y}_1^l, \dots, \mathbf{y}_{N_L}^l]) = \sum_{i=1}^{N_L} (\mathbf{y}_i^l - \mathbf{t}_i^p)^2 \quad (3)$$

To find the derivative of the MSE, Δ_k^l is utilized for updating the bias of that neuron and all weights of the neurons in the preceding layer:

$$\frac{\partial E}{\partial \mathbf{w}_{ik}^{l-1}} = \Delta_k^l \mathbf{y}_i^{l-1} \quad \text{and} \quad \frac{\partial E}{\partial \mathbf{b}_k^l} = \Delta_k^l \quad (4)$$

Then, the regular back-propagation is calculated as:

$$\frac{\partial E}{\partial \mathbf{s}_k^l} = \Delta \mathbf{s}_k^l = \sum_{i=1}^{N_{l+1}} \frac{\partial E}{\partial \mathbf{x}_i^{l+1}} \frac{\partial \mathbf{x}_i^{l+1}}{\partial \mathbf{s}_k^l} = \sum_{i=1}^{N_{l+1}} \Delta_i^{l+1} \mathbf{w}_{ki}^l \quad (5)$$

Further back-propagation to the input delta, Δ_k^l :

Table 1Technical specification of TROMINO[®] ENGY wireless sensing units.

Dimensions	10 × 7 × 13 cm
Weight	1 kg
Storage capacity	4 GB
Standard frequency band	0.1–500 Hz
Velocimetric channels	3 velocimetric channels for seismic ambient microtremor and strong vibrations, 6 amplification levels (saturation from ± 1.2 mm/s to ± 50 mm/s in band)
Accelerometric channels	(± 2 g, background noise $\sim \pm 40$ μ g, signal detection threshold $\sim \pm 100$ μ g) (final output from 4 accelerometers x 3 axes)
Analog channels	1 analog channel
Sampling rates	128, 256, 512, 1024 Hz on all channels
GPS	Built-in GPS module with internal or external antenna
Radio	Built-in radio module for indoor and outdoor synchronization of several TROMINO [®] ENGY units.

**Fig. 3.** Two girders instrumented with ten wireless units.**Fig. 4.** Wireless unit attached to the girder top flange.

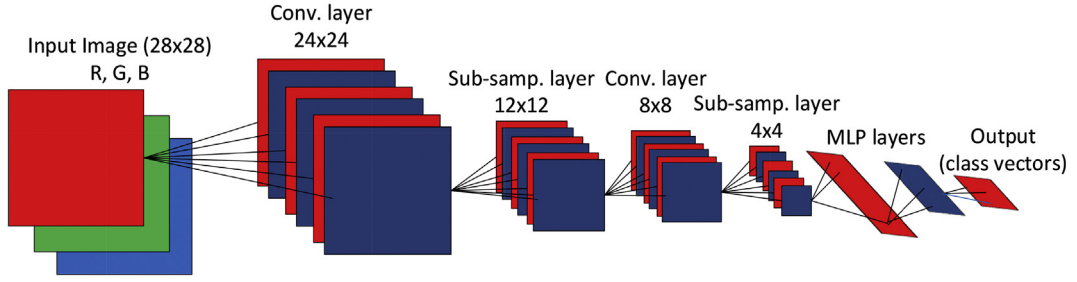


Fig. 5. A sample conventional CNN.

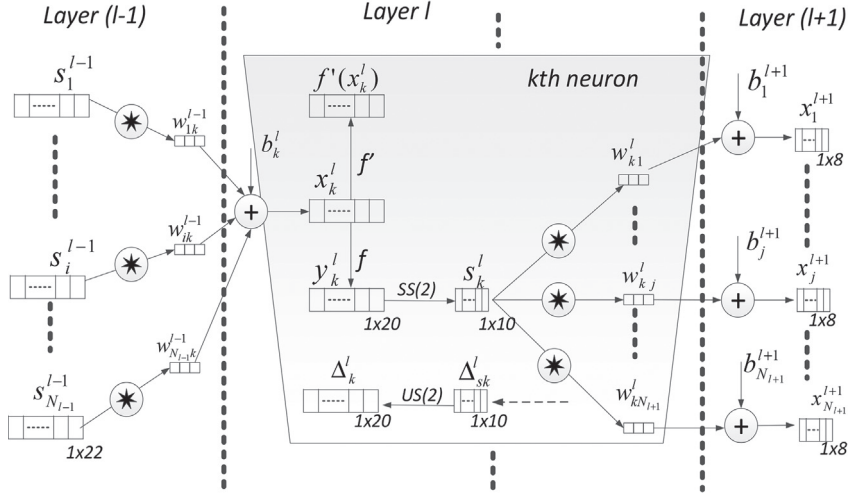


Fig. 6. Proposed adaptive 1D CNN setup: The convolution layers.

$$\Delta_k^l = \frac{\partial E}{\partial y_k^l} \frac{\partial y_k^l}{\partial x_k^l} = \frac{\partial E}{\partial s_k^l} \frac{\partial s_k^l}{\partial y_k^l} f'(x_k^l) = \text{up}(\Delta_k^l) \beta f'(x_k^l) \quad (6)$$

where $\beta = (ss)^{-1}$.

Then, the BP of the delta error ($\Delta_k^l \xrightarrow{\Sigma} \Delta_k^{l+1}$) can be expressed as:

$$\Delta s_k^l = \sum_{i=1}^{N_{l+1}} \text{conv 1Dz}(\Delta_i^{l+1}, \text{rev}(w_{ki}^l)) \quad (7)$$

where $\text{rev}(\cdot)$ is used to reverse the array and $\text{conv 1Dz}(\cdot, \cdot)$ is used to perform full convolution in 1D. As such, the weight and bias sensitivities are written:

$$\frac{\partial E}{\partial w_{ik}^l} = \text{conv 1D}(\Delta_k^l, \Delta_i^{l+1}) \quad \text{and} \quad \frac{\partial E}{\partial b_k^l} = \sum_n \Delta_k^l(n) \quad (8)$$

The pattern of the BP algorithm is shown more in detail in Refs. [33,65]. The flow results in updating the biases and weights where the sensitivities scaled with the learning factor, ϵ as:

$$w_{ik}^{l-1}(t+1) = w_{ik}^{l-1}(t) - \epsilon \frac{\partial E}{\partial w_{ik}^{l-1}} \quad (9)$$

$$b_k^l(t+1) = b_k^l(t) - \epsilon \frac{\partial E}{\partial b_k^l} \quad (10)$$

6. The proposed method for structural damage detection and localization

In this work, the structural damage is introduced by simply loosening the bolts connecting the filler beams to the main girders. The main goal of the 1D CNN-based SDD algorithm is to sense the structural damage (if any) and determine the location of the damaged joint(s). Also, as mentioned earlier, the proposed damage detection method will take into account the response along the three directions at each joint in order to find the direction along which the damage features are more distinguishable. Therefore, it is required to design and train three 1D CNNs for each one of the monitored 10 joints. Each CNN is responsible for assessing the condition of one joint along a particular direction using only the raw velocity signal measured by the wireless sensor at this joint. Therefore, the proposed damage detection algorithm is decentralized since each CNN is capable of detecting damage at its respective joint independently from the other CNNs. Moreover, each CNN is trained based only on the acceleration signals measured at its corresponding location independently from the measurements obtained at the other locations. Hence, the CNN training process is also decentralized.

6.1. CNN training

The training process of the CNNs involves generating a data set consisting of a number of undamaged/damaged acceleration signals for each joint of the monitored structure. For a structure having a total of n monitored joints as shown in Fig. 7, a unique CNN is assigned to each principal direction of each joint, resulting in a total of $3n$ CNNs. This means, for generating the training data set needed to train the CNNs, it is required to conduct $n + 1$ experiments. In the first experiment ($E = 1$), the triaxial sensors are used to measure the $3n$ vibration signals for the *undamaged* structure (i.e. when all joints are undamaged) under ambient conditions, along the Z, NS, and EW directions.

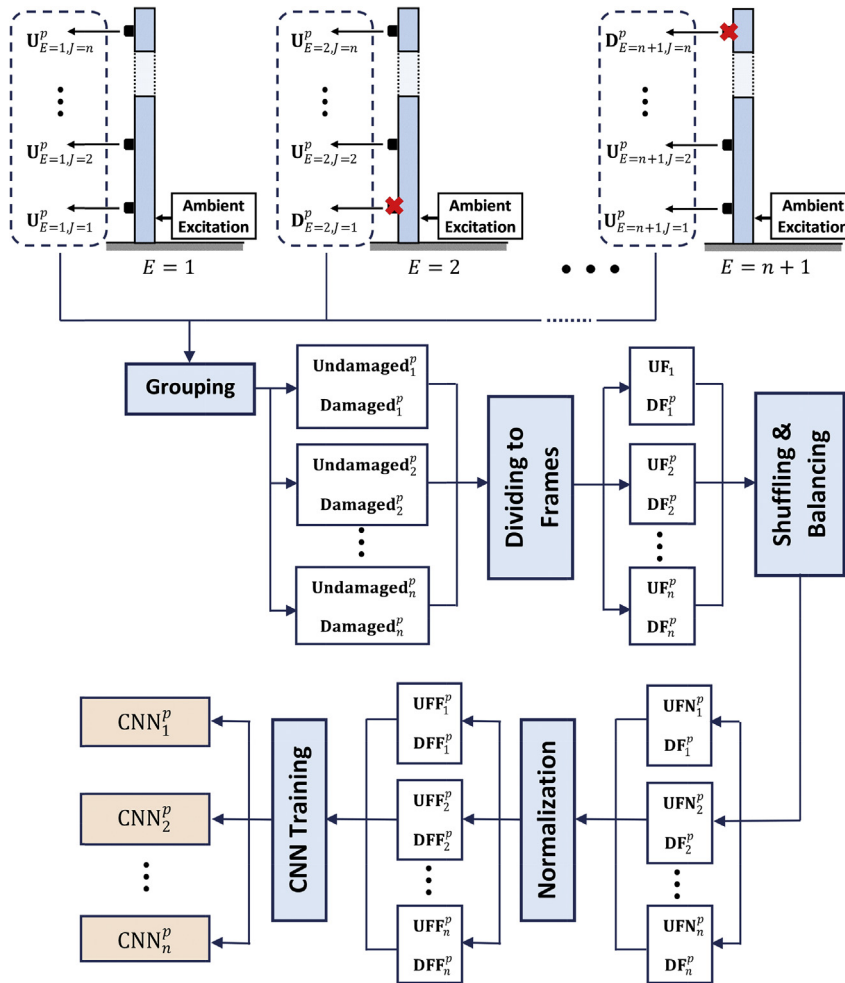


Fig. 7. Data generation and CNN training process for a particular direction p (the damaged joints are marked with a red-cross). (For interpretation of the references to color in this figure legend, the reader is referred to the Web version of this article.)

The resulting signals are denoted as $\mathbf{U}_{E=1,J=1}^{p=1}, \dots, \mathbf{U}_{E=1,J=n}^{p=1}, \mathbf{U}_{E=1,J=1}^{p=2}, \dots, \mathbf{U}_{E=1,J=n}^{p=2}, \mathbf{U}_{E=1,J=1}^{p=3}, \dots, \mathbf{U}_{E=1,J=n}^{p=3}$. The notation \mathbf{U} shows that the signal is measured at an undamaged joint, whereas the subscripts E denotes the experiment number and J denotes the joint number. Also, the superscript p indicates the direction at which the signals were measured, where $p = 1, 2, 3$ denote the Z, NS, and EW directions, respectively. As a following step, the remaining experiments are conducted one by one, in a sequential order, as explained below.

In each experiment, $E = k + 1$, damage is introduced at the joint $J = k$ (by loosening the filler beam connection bolts in this study). $3n$ acceleration signals are measured under ambient conditions of the laboratory environment.

The measured signal data are represented as $\mathbf{U}_{E=k+1,J=1}^{p=1,2,3}, \dots, \mathbf{D}_{E=k+1,J=k}^{p=1,2,3}, \mathbf{U}_{E=k+1,J=n}^{p=1,2,3}$ with the D showing that this signal was measured at the damaged joint k . Running $n + 1$ experiments, the signals measured at each joint i along each direction p are grouped together as follows in order to form the damaged/undamaged vectors needed to train the corresponding CNN, CNN_i^p :

$$\mathbf{Undamaged}_i^p = \left[\mathbf{U}_{E=1,J=i}^p \quad \mathbf{U}_{E=2,J=i}^p \quad \dots \quad \mathbf{U}_{E=i,J=i}^p \quad \mathbf{U}_{E=i+2,J=i}^p \quad \dots \quad \mathbf{U}_{E=n+1,J=i}^p \right] \quad (11)$$

$$\mathbf{Damaged}_i^p = \left[\mathbf{D}_{E=i+1,J=i}^p \right] \quad (12)$$

It should be noted that the undamaged data set for a particular joint i along a specific direction p includes signals measured while the other joints are undamaged ($\mathbf{U}_{E=1,J=i}^p$) as well as signals measured while one of the other joints are damaged. The data generation and collection process was conducted this way to minimize the effect of damaged joints on the classification efficiency of the CNNs at the other joints. The intent with that was to make sure that the effect of damaging a particular joint on the response of the other joints will not cause the CNNs to misclassify the undamaged joints as damaged.

The following step is to divide the aforementioned undamaged and damaged vectors to a large number of frames, where each frame is made up of a certain number of samples n_s . The result of this operation for joint i can be written as:

$$\mathbf{UF}_i^p = \left[\mathbf{UF}_{i,1}^p \quad \mathbf{UF}_{i,2}^p \quad \dots \quad \mathbf{UF}_{i,n_{uf}}^p \right] \quad (13)$$

$$\mathbf{DF}_i^p = \left[\mathbf{DF}_{i,1}^p \quad \mathbf{DF}_{i,2}^p \quad \dots \quad \mathbf{DF}_{i,n_{df}}^p \right] \quad (14)$$

where \mathbf{UF}_i^p is a vector that contains the undamaged frames for the joint i and \mathbf{DF}_i^p is a vector that contain damaged frames for along direction p . Meanwhile, n_{uf} is the total number of undamaged and n_{df} is the total number of damaged frames. As such, with the total number of samples in each acceleration signal n_T , then, n_{uf} and n_{df} can be computed as:

$$n_{uf} = n \times \frac{n_T}{n_s} \quad (15)$$

$$n_{df} = \frac{n_T}{n_s} \quad (16)$$

Observing Equations (15) and (16), it is clear that in a structure containing a large number of joints n , the number of undamaged frames for a particular joint along a specific direction will be significantly larger than the number of damaged frames. Meanwhile, training the CNN using extremely unbalanced undamaged/damaged frames may degrade the classification performance. Thus, the frames corresponding to joint i along direction p are balanced according to the following procedure:

1. The n_{uf} frames in \mathbf{UF}_i^p are randomly shuffled to yield a new vector, \mathbf{UFS}_i^p .
2. The shuffled vector \mathbf{UFS}_i^p is truncated by taking only the first n_{df} and remove the remaining frames resulting in a new undamaged vector \mathbf{UFN}_i^p that contains a total of n_{df} frames.

It must be emphasized that \mathbf{UF}_i^p was shuffled to make sure that the undamaged frames from all experiments have an equal chance of being selected. At the same time, all frames in vectors \mathbf{UFN}_i^p and \mathbf{DF}_i^p are normalized to form final vectors \mathbf{UFF}_i^p and \mathbf{DFF}_i^p . These frames are broken down into training frames and testing frames. The training frames, as the name implies, are utilized to train the CNN, CNN_i^p , while the testing frames are used to evaluate its performance as will be explained in Section 6.2.

For the training of CNN_i^p , it is required to specify its parameters such as the number of convolutional layers and neurons, the number of hidden fully-connected layers and neurons, the sub-sampling factor (ss), as well as the kernel size (K). The training of the CNN is performed based on the corresponding training frames using back-propagation as explained above. The entire data generation and CNN training process for a particular direction p is shown in Fig. 7.

6.2. Obtaining the best CNN

As explained above, a total of $3n$ CNNs have been trained (i.e. three CNNs per joint, corresponding to the three principal directions). The next step is to test all the CNNs in order to find out which CNN has the best performance at each joint. This would also indicate the direction along which the damage features are more distinguishable. For example, if the test showed $\text{CNN}_{i=1}^{p=1}$ is performing better than $\text{CNN}_{i=1}^{p=2}$ and $\text{CNN}_{i=1}^{p=3}$, it would be clear that the damage induced at the joint $i = 1$ has more significant effect on the response along the Z direction than on the other two directions. The testing procedure is summarized as follows:

1. Feed each CNN, CNN_i^p with the corresponding testing frames (generated previously as explained in Section 6.1).
2. Compute the classification error of each CNN, CNN_i^p as:

$$\text{CE}_i^p = \frac{M_i^p}{T_i^p} \quad (17)$$

where T_i^p is the total number of frames processed by CNN_i^p , and M_i^p is the number of misclassified frames.

- 3 For each joint i , select the best CNN_i^p that produced the lowest classification error.
- 4 The best CNN for each joint is saved in order to be utilized for SDD as will be explained in Section 6.3, while the other CNNs are discarded. This will result in n CNNs only (i.e. one CNN per joint). These CNNs are denote as $\text{CNN}_1, \text{CNN}_2, \dots, \text{CNN}_n$.

6.3. Using the CNNs for damage detection

When all the n best CNNs are determined based on the procedure detailed in Sections 6.1 and 6.2, they can be directly utilized to find out the condition of the monitored structure. Each CNN_i is utilized to compute an index that reflects the likelihood of damage at joint i through the raw vibration signal measured at its location along its corresponding direction. This can be done according to the following steps:

1. Induce damage at one or more locations (or keep the structure undamaged).
2. Measure the three vibration signals at each joint along the three directions.
3. For each joint, keep the signal corresponding to the direction at which the best CNN was trained and discard the other two signals.
4. Break down each vibration signal into a number of frames each containing a total of n_s samples.
5. Do the normalization of the frames between -1 and 1 .
6. At each joint to the corresponding CNN (CNN_i), feed the normalized frames
7. Calculate the probability of damage (PoD_i) at the i^{th} joint as below:

$$\text{PoD}_i = \frac{D_i}{T_i} \quad (18)$$

where T_i is the total number of frames processed by CNN_i , and D_i is the number of frames classified as “damaged”. As will be verified experimentally in Section 7, the PoD computed at damaged joints are expected to be significantly higher than the values for the undamaged joints. This would give a good idea for the presence (if any) and the location of a structural damage.

7. Experimental results

The efficiency of the proposed 1D CNN-based SDD algorithm is evaluated utilizing QUGS. The two horizontal girders marked in Fig. 1 were equipped with 10 triaxial wireless sensor units (i.e. one unit at each beam-to-girder joint). As explained in Section 6.1, a total of 11 experiments were run to generate the data required for training. In each experiment, the velocity signals were collected at each joint along the three-principal directions under ambient excitations. The signals were recorded for 240 s at a sampling frequency of 1024 Hz, therefore, each signal contains $n_T = 245760$ samples. A Matlab [71] code (explained in Section 7.1) is used to group, divide into frames, balance, and normalize the data sets. The frame length n_s was taken as 512 samples, therefore, vectors \mathbf{UFF}_i^p and \mathbf{DFF}_i^p contain a total of 480 frames for each joint i along each direction p . 85% of these frames were used for the training process (i.e. 408 undamaged frames and 408 damaged frames for each CNN), while the remaining 15% were used for evaluating the CNNs.

30 CNNs were trained for the 10 joints along the tested girders. All the CNNs were selected to have two hidden convolution layers and two hidden fully-connected layers. The aim for such a compact configuration was to accomplish a high computational efficiency required particularly in wireless sensor networks. The structure and parameters of the 1D CNNs were obtained by trial-and-error. The 1D CNN structure of all experiments has (5, 5) neurons on the two hidden convolution layers and (4, 4) neurons on the two hidden fully-connected layers. The size of the MLP is 2 (equal to the number of classes). Also, each CNN has a single input neuron taking the input signal as the 512 time-domain data point for each frame in the training set. The kernel size K is set to 80 and the ss is 2 for all CNNs.

For the entire experiments, the following stopping criteria for BP training was assigned:

- 1 The train classification error (CE) of 1%.
- 2 Maximum 200 BP iterations.

At the time either criterion is satisfied, the training of the BP terminates. At the beginning, the learning factor, ϵ , is set as 0.001. At each iteration, if the trained MSE decreases in the previous iteration, then the learning factor is increased by 5%; if not, it is decreased by 30%.

After finishing the training of the 30 CNNs, their performance was assessed using the remaining 15% of the collected data as explained in Section 6.2. The classification errors of the 30 CNNs are plotted in Fig. 8. Looking at the Figure, it is obvious that the CNNs performance significantly depends on the direction of measurement. For the joints 2 to 9, the CNNs corresponding to the Z direction performed better than the others. This indicates that the effect of the damaged induced at these joints on their vibration response is more significant along the Z direction. On the other hand, for the 1st joint, the performance was better along the NS direction. The performance of the all CNNs corresponding to the EW direction was generally poor, which indicates that the damage features are not distinguishable along the axial direction of the girders.

Next, the best CNN at each joint was selected as shown in Fig. 8. In an attempt to measure the success of the proposed 1D CNN-based algorithm, the process explained in Section 6.3 was conducted for a total of 11 damage cases, where Case 1 to the undamaged girders, while Cases 2 to 11 correspond to loosening a single joint as shown in Fig. 9. By processing the raw signals based on the CNN-based algorithm, the 11 PoD distributions shown in Fig. 10 were obtained.

Overall, the results of the experimental work clearly demonstrate a significant achievement of the proposed SDD algorithm in assessing the condition of structures and locating the damaged joint. For all 11 scenarios, the PoD values obtained by processing the raw ambient vibration signals by the 10 CNNs clearly indicate the location of damage. The PoD results shown in Fig. 10 are observed to be an evident success considering the fact that this is a pioneer application of 1D CNNs on WSNs for SDD purposes. The SDD is successfully performed completely wireless and real-time under ambient conditions.

Starting from Case 1 (i.e. the undamaged structure), the algorithm has successfully assigned very low PoD values (close to zero) to all ten joints. For the other damage cases (i.e. Case 2 to 11), the damage detection algorithm has successfully assigned high PoD values (higher than 0.85) to the damaged joints and lower PoD values to the undamaged ones.

7.1. Computational complexity analysis

The adaptive 1D CNN classifier explained in Section 4.1 is implemented in C++ using MS Visual Studio 2013 in 64-bit. This program is capable of carrying out the forward and back-propagation tasks required for training and using the CNNs. Also, a

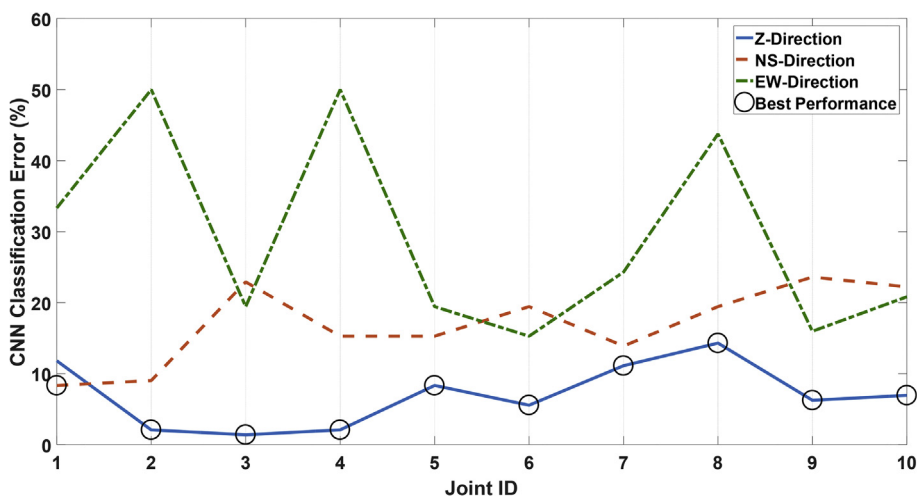


Fig. 8. Classification performance of the 30 CNNs.

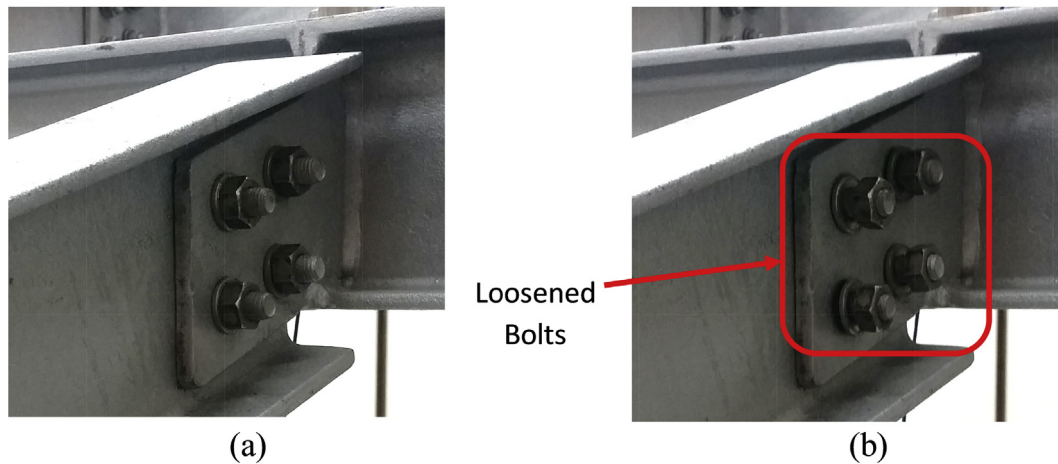


Fig. 9. (a) Undamaged joint. (b) Damaged joint.

Matlab [71] code was developed and utilized to extract vectors UFF_i and DFF_i directly from the signals collected in the experiments as detailed in Section 5.1. Another Matlab code was used to generate the PoD distribution directly from the raw acceleration signals using the trained CNNs as explained in Section 5.2. The experiments were conducted using a computer with I7-4910MQ at 2.9 GHz (8 cores) and 32-Gb memory.

As mentioned earlier, the key feature of the proposed CNN-based damage detection technique is that the computational time and power required to classify the signals are significantly reduced. This is particularly crucial in wireless SHM since the power of the wireless units is usually limited. To illustrate this feature, the same CNN configuration has been used. The acceleration signal used for this illustration was acquired at a sampling frequency of 1024 Hz; therefore, it consists of 1024 samples. The signal was divided to two frames each having 512 samples. Accordingly, the total time required for the classification of 1-sec signal was only 27 msec. Note that this speed is about $37 \times$ faster than the real-time requirement.

8. Conclusions

In this paper, the authors presented an application of 1D CNNs on wireless sensor networks for structural damage detection purposes. The SDD is successfully performed completely wirelessly and in real-time, under ambient conditions. The proposed method is decentralized and computationally-inexpensive; and it is capable of extracting damage indices that reflect the health of the monitored structure directly through the raw ambient vibration conditions.

The efficiency of the damage detection system was verified experimentally using a large-scale laboratory structure instrumented with wireless sensing units. Based on the experimental results presented in this study, the following conclusions can be drawn:

- The CNNs are capable of learning directly from the raw vibration data measured under ambient excitations. Therefore, the proposed algorithm is very promising for monitoring of large civil structures where applying an artificial excitation (e.g. with a shaker) is almost impossible.
- Processing the vibration data using 1D CNNs involves only simple 1D operations (scalar multiplications and additions). Therefore, as shown in the computational complexity analysis, the proposed CNN-based method is computationally inexpensive, which makes it suitable for wireless SHM applications.
- The conventional centralized algorithms require the signals measured at all locations to be collected and transferred to a single processing unit. Transferring and synchronizing large amount of data can be problematic especially when a WSN is used for SHM. The proposed algorithm is decentralized, which means that an individual classifier (CNN) is assigned to each location. Each CNN processes only the locally-available data to assess the structural condition at its location. Hence, the proposed method offers an efficient and feasible solution to overcome this problem.
- In this study, the CNN-based damage detection algorithm proposed by the authors in Ref. [33] was improved in order to enable it to analyze the vibration response along the three directions and find the direction along which the damage features are more distinctive. The experimental results demonstrated that this modification has resulted in lower classification error of 1D CNNs, and therefore better damage detection performance. Considering the fact that all damage detection processes of this paper were performed under ambient excitations, the superiority of the proposed method becomes even more obvious.

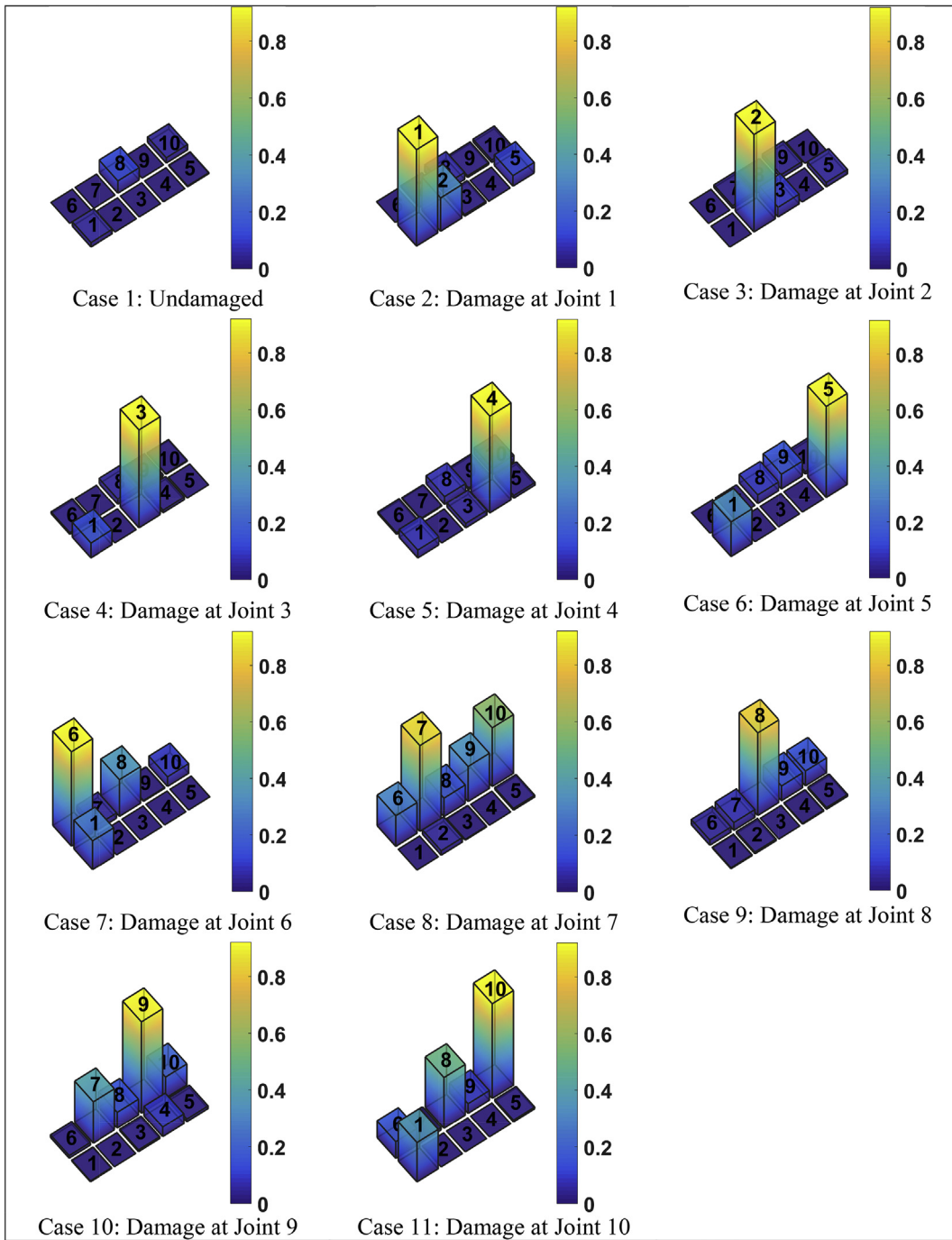


Fig. 10. PoD distributions for Cases 1–11.

Finally, the following issues should be addressed in future studies in order to improve the proposed damage detection method and overcome its limitations:

1. In this paper, measurements from 11 structural scenarios (1 undamaged + 10 damage cases) were required to train the 10 CNNs. The authors are currently developing an alternative method for generating the data needed for CNN training that requires significantly lower number of structural scenarios. This will make the proposed method more applicable for real structures where testing the structure under several damage scenarios is not feasible.

2. The proposed method requires real damaged data measured under real damage cases in order to train the CNNs required for damage detection. Since such data is very difficult to obtain for civil structures, the authors are currently investigating whether it is possible to train the CNNs using simulated damaged data generated by finite element simulations.
3. In this paper, the damage detection method was tested only under joint damage cases. It is recommended to test the proposed method under a wider range of damage cases such as stiffness and mass changes in the beams.
4. Finally, it is important to note that the proposed method is only applicable in the cases where structural damage cases are anticipated and can be tested for. Further studies are recommended to overcome this limitation.

References

- [1] J.M.W. Brownjohn, Structural health monitoring of civil infrastructure, *Struct. Heal. Monit. Civ. Infrastruct.* (2007), <https://doi.org/10.1098/rsta.2006.1925>.
- [2] C.R. Farrar, K. Worden, An introduction to structural health monitoring, *Philos. Trans. R. Soc. A* (2007), <https://doi.org/10.1098/rsta.2006.1928>.
- [3] K. Worden, G. Manson, S. Rippengill, *Structural Health Monitoring of Civil Infrastructure Systems*, 2009, <https://doi.org/10.1533/9781845696825.1.305>.
- [4] O. Avci, O. Abdeljaber, Self-organizing maps for structural damage detection: a novel unsupervised vibration-based algorithm, *J. Perform. Constr. Facil.* 30 (2016), [https://doi.org/10.1061/\(ASCE\)CF.1943-5509.0000801](https://doi.org/10.1061/(ASCE)CF.1943-5509.0000801).
- [5] J. Ou, H. Li, *Structural Health Monitoring of Civil Infrastructure Systems*, 2009, <https://doi.org/10.1533/9781845696825.2.463>.
- [6] M.I. Friswell, S. Adhikari, Structural health monitoring using shaped sensors, *Mech. Syst. Signal Process.* (2010), <https://doi.org/10.1016/j.ymssp.2009.10.009>.
- [7] O. Abdeljaber, O. Avci, Nonparametric structural damage detection algorithm for ambient vibration response: utilizing artificial neural networks and self-organizing maps, *J. Archit. Eng.* (2016), [https://doi.org/10.1061/\(ASCE\)AE.1943-5568.0000205](https://doi.org/10.1061/(ASCE)AE.1943-5568.0000205).
- [8] F.N. Catbas, O. Celik, O. Avci, O. Abdeljaber, M. Gul, N.T. Do, Sensing and monitoring for stadium structures: a review of recent advances and a forward look, *Front. Built Environ* 3 (2017) 38, <https://doi.org/10.3389/fbuil.2017.00038>.
- [9] Q.H. Jia He, You-Lin Xu, Sheng Zhan, Structural control and health monitoring of building structures with unknown ground excitations: experimental investigation, *J. Sound Vib.* 390 (2017) 23–38, <https://doi.org/10.1016/j.jsv.2016.11.035>.
- [10] K.W.N. Dervilis, E.J. Cross, R.J. Barthorpe, Robust methods of inclusive outlier analysis for structural health monitoring, *J. Sound Vib.* 333 (2014) 5181–5195, <https://doi.org/10.1016/j.jsv.2014.05.012>.
- [11] A.B.T.H. Loutas, Strain sensors optimal placement for vibration-based structural health monitoring. The effect of damage on the initially optimal configuration, *J. Sound Vib.* 410 (2017) 217–230, <https://doi.org/10.1016/j.jsv.2017.08.022>.
- [12] B.F. Spencer, H. Jo, K.A. Mechitov, J. Li, S.H. Sim, R.E. Kim, S. Cho, L.E. Linderman, P. Moizadeh, R.K. Giles, G. Agha, Recent advances in wireless smart sensors for multi-scale monitoring and control of civil infrastructure, *J. Civ. Struct. Heal. Monit.* (2016), <https://doi.org/10.1007/s13349-015-0111-1>.
- [13] F. Ansari, Practical implementation of optical fiber sensors in civil structural health monitoring, *J. Intell. Mater. Syst. Struct.* (2007), <https://doi.org/10.1177/1045389X060075760>.
- [14] A.H. Alavi, H. Hasni, N. Lajnef, K. Chatti, F. Faridazar, Damage detection using self-powered wireless sensor data: an evolutionary approach, *Measurement* 82 (2016) 254–283, <https://doi.org/10.1016/j.measurement.2015.12.020>.
- [15] M. Wang, J. Cao, B. Chen, Y. Xu, J. Li, Distributed processing in wireless sensor networks for structural health monitoring, *Ubiquitous Intell. Comput.* (2007), <https://doi.org/10.1007/978-3-540-73549-6>.
- [16] S. Kim, S. Pakzad, D. Culler, J. Demmel, G. Fenves, S. Glaser, M. Turon, *Wireless Sensor Networks for Structural Health Monitoring*, 2006, <https://doi.org/10.1145/1031495.1031498>.
- [17] T.L. Kijewski-Correa, M. Haenggi, P. Antsaklis, Multi-scale wireless sensor networks for structural health monitoring, in: *Proc. 2nd Int. Conf. Struct. Heal. Monit. Intell. Infrastruct.*, 2005.
- [18] Y. Wang, *Wireless Sensing and Decentralized Control for Civil Structures: Theory and Implementation*, Stanford University, 2007.
- [19] R. Klis, E.N. Chatzi, Vibration monitoring via spectro-temporal compressive sensing for wireless sensor networks, *Struct. Infrastruct. Eng.* 13 (2017) 195–209, <https://doi.org/10.1080/15732479.2016.1198395>.
- [20] T.-Y. Hsu, S.-K. Huang, K.-C. Lu, C.-H. Loh, Y. Wang, J.P. Lynch, On-line structural damage localization and quantification using wireless sensors, *Smart Mater. Struct.* 20 (2011) 105025, <https://doi.org/10.1088/0964-1726/20/10/105025>.
- [21] R. Klis, E. Chatzi, V. Dertimanis, Experimental validation of spectro-temporal compressive sensing for vibration monitoring using wireless sensor networks, in: *Life-cycle Eng. Syst. Emphas. Sustain. Civ. Infrastruct. - 5th Int. Symp. Life-cycle Eng. IALCEE 2016*, 2017, <https://doi.org/10.1201/9781315375175-91>.
- [22] M. Mihaylov, K. Tuyts, A. Nowé, Decentralized learning in wireless sensor networks, in: *Belgian/Netherlands Artif. Intell. Conf*, 2009, pp. 345–346, https://doi.org/10.1007/978-3-642-11814-2_4.
- [23] Y. Wang, J.P. Lynch, K.H. Law, A wireless structural health monitoring system with multithreaded sensing devices: design and validation, *Struct. Infrastruct. Eng.* 3 (2007) 103–120, <https://doi.org/10.1080/15732470600590820>.
- [24] E.G. Straser, A.S. Kiremidjian, T.H. Meng, L. Redlfeisen, A modular, wireless network platform for monitoring structures, in: *16th International Modal Anal. Conf.*, 1998, pp. 450–456, [https://doi.org/10.1016/S0920-5489\(99\)91996-7](https://doi.org/10.1016/S0920-5489(99)91996-7).
- [25] S. Park, C.-B. Yun, D.J. Inman, G. Park, Wireless structural health monitoring for critical members of civil infrastructures using piezoelectric active sensors, in: *Proc. SPIE - Int. Soc. Opt. Eng.*, 2008, <https://doi.org/10.1117/12.784990>.
- [26] X.M. Wang, G. Foliente, Z.Q. Su, L. Ye, Multilevel decision fusion in a distributed active sensor network for structural damage detection, *Struct. Heal. Monit. Int. J.* (2006), <https://doi.org/10.1177/14759217060057981>.
- [27] Z. Su, L. Ye, An intelligent signal processing and pattern recognition technique for defect identification using an active sensor network, *Smart Mater. Struct.* (2004), <https://doi.org/10.1088/0964-1726/13/4/034>.
- [28] A. Noel, A. Abdaoui, A. Badawy, T. Elfouly, M. Ahmed, M. Shehata, Structural health monitoring using wireless sensor networks: a comprehensive survey, *IEEE Commun. Surv. Tutorials* (2017), <https://doi.org/10.1109/COMST.2017.2691551>.
- [29] M. Elersy, T.M. Elfouly, M.H. Ahmed, Joint Optimal Placement, Routing, Flow Assignment, In wireless sensor networks for structural health monitoring, *IEEE Sens. J.* (2016), <https://doi.org/10.1109/JSEN.2016.2554462>.
- [30] S.F. Ghahari, F. Abazarsa, O. Avci, M. Çelebi, E. Taciroglu, Blind identification of the Millikan Library from earthquake data considering soil-structure interaction, *Struct. Control Heal. Monit.* (2016), <https://doi.org/10.1002/stc.1803>.
- [31] R.A. Swartz, in: M. Garevski (Ed.), *Decentralized Algorithms for SHM over Wireless and Distributed Smart Sensor Networks BT - Earthquakes and Health Monitoring of Civil Structures*, Springer Netherlands, Dordrecht, 2013, pp. 109–131 doi: 10.1007/978-94-007-5182-8_4.
- [32] D. Zhou, D.S. Ha, D.J. Inman, Ultra low-power active wireless sensor for structural health monitoring, *Smart Struct. Syst.* (2010), https://doi.org/10.12989/sss.2010.6.5_6.675.
- [33] O. Abdeljaber, O. Avci, S. Kiranyaz, M. Gabbouj, D.J. Inman, Real-time vibration-based structural damage detection using one-dimensional convolutional neural networks, *J. Sound Vib.* 388 (2017) 154–170, <https://doi.org/10.1016/j.jsv.2016.10.043>.
- [34] H.L. Guolin He, Kang Ding, Fault feature extraction of rolling element bearings using sparse representation, *J. Sound Vib.* 366 (2016) 514–527, <https://doi.org/10.1016/j.jsv.2015.12.020>.

- [35] X.D. Qingbo He, Sparse representation based on local time–frequency template matching for bearing transient fault feature extraction, *J. Sound Vib.* 370 (2016) 424–443, <https://doi.org/10.1016/j.jsv.2016.01.054>.
- [36] B.T. Yi Qin, Yi Tao, Ye He, Adaptive bistable stochastic resonance and its application in mechanical fault feature extraction, *J. Sound Vib.* 333 (2014) 7386–7400, <https://doi.org/10.1016/j.jsv.2014.08.039>.
- [37] O. Avci, O. Abdeljaber, S. Kiranyaz, D. Inman, Structural damage detection in real time: implementation of 1d convolutional neural networks for SHM applications, in: C. Niezrecki (Ed.), *Structural Health Monitoring & Damage Detection*, Conference Proceedings of the Society for Experimental Mechanics Series, vol. 7, Springer, Cham, 2017, pp. 49–54, https://doi.org/10.1007/978-3-319-54109-9_6, 2017.
- [38] J.P. Lynch, K.J. Loh, A summary review of wireless sensors and sensor networks for structural health monitoring, *Shock Vib. Dig* (2006), <https://doi.org/10.1177/05831024060061499>.
- [39] A. Noel, A. Abdaoui, A. Badawy, T. Elfouly, M. Ahmed, M. Shehata, Structural health monitoring using wireless sensor networks: a comprehensive survey, *IEEE Commun. Surv. Tutorials* (2017), <https://doi.org/10.1109/COMST.2017.2691551>.
- [40] J. Paek, K. Chintalapudi, A wireless sensor network for structural health monitoring: performance and experience, *Netw. Sens* (2005), <https://doi.org/10.1109/EMNETS.2005.1469093>.
- [41] B. Chen, W. Liu, Mobile agent computing paradigm for building a flexible structural health monitoring sensor network, *Comput. Civ. Infrastruct. Eng* (2010), <https://doi.org/10.1111/j.1467-8667.2010.00656.x>.
- [42] D. Musiani, K. Lin, T.S. Rosing, Active sensing platform for wireless structural health monitoring, in: *IPSN '07 Proc. 6th Int. Conf. Inf. Process. Sens. Networks*, 2007, <https://doi.org/10.1109/IPSN.2007.4379699>.
- [43] S. Jang, H. Jo, S. Cho, K.A. Mechitov, J.A. Rice, S.-H. Sim, H.J. Jung, C.-B. Yun, B.F. Spencer Jr., G. Agha, Structural health monitoring of a cable-stayed bridge using smart sensor technology: deployment and evaluation, *Smart Struct. Syst.* 6 (2010) 439–459.
- [44] M. Bocca, E.I. Cosar, J. Salminen, L.M. Eriksson, A reconfigurable wireless sensor network for structural health monitoring, in: *Proc. 4th Int. Conf. Struct. Heal. Monit. Intell. Infrastruct.*, 2009.
- [45] X. Liu, J. Cao, W.-Z. Song, S. Tang, Distributed sensing for high quality structural health monitoring using wireless sensor networks, in: *Real-time Syst. Symp. (RTSS)*, 2012 IEEE 33rd, 2012, <https://doi.org/10.1109/RTSS.2012.60>.
- [46] V.A. Kottapalli, A.S. Kiremidjian, J.P. Lynch, E. Carryer, T.W. Kenny, K.H. Law, Y. Lei, Two-tiered wireless sensor network architecture for structural health monitoring, in: *Proc. SPIE - Int. Soc. Opt. Eng.*, 2003, <https://doi.org/10.1117/12.482717>.
- [47] D.D.L. Mascarenas, E.B. Flynn, M.D. Todd, T.G. Overly, K.M. Farinholt, G. Park, C.R. Farrar, Development of capacitance-based and impedance-based wireless sensors and sensor nodes for structural health monitoring applications, *J. Sound Vib.* 329 (2010) 2410–2420, <https://doi.org/10.1016/j.jsv.2009.07.021>.
- [48] S.T. Quek, V. a. Tran, X.Y. Hou, W.H. Duan, Structural damage detection using enhanced damage locating vector method with limited wireless sensors, *J. Sound Vib.* 328 (4–5) (2009) 411–427, <https://doi.org/10.1016/j.jsv.2009.08.018>.
- [49] X.J.X. Jiang, Y.T.Y. Tang, Y.L.Y. Lei, Wireless sensor networks in structural health monitoring based on ZigBee technology, in: *2009 3rd Int. Conf. Anti-counterfeiting, Secur. Identif. Commun.*, 2009, <https://doi.org/10.1109/ICASID.2009.5276977>.
- [50] M. Bocca, J. Toivola, L.M. Eriksson, J. Hollmén, H. Koivo, Structural health monitoring in wireless sensor networks by the embedded goertzel algorithm, in: *Proc. 2nd ACM/IEEE Int. Conf. Cyber-physical Syst. - ICCPS '11*, 2011, <https://doi.org/10.1109/ICCPS.2011.19>.
- [51] Y. Bao, H. Li, X. Sun, Y. Yu, J. Ou, Compressive sampling–based data loss recovery for wireless sensor networks used in civil structural health monitoring, *Struct. Heal. Monit. An Int. J* (2013), <https://doi.org/10.1177/1475921712462936>.
- [52] M.J.T. Thirumurthy, F.M. Mustapha, A.H.S. Shirazi, M.K.H. Muda, Wireless Structural Health Monitoring (SHM) system for damage detection using ultrasonic guided waveform response, *Pertanika J. Sci. Technol* 25 (2017) 283–292.
- [53] M.-X. Xie, H.-N. Li, Guang-Dong Zhou, Ting-hua Yi, Wireless sensor placement for structural monitoring using information-fusing firefly algorithm, *Struct. Mater. Struct.* 26 (10) (2017), <https://doi.org/10.1088/1361-665X/aa7930>.
- [54] H. Wang, X.J. Jing, Fault diagnosis of sensor networked structures with multiple faults using a virtual beam based approach, *J. Sound Vib.* 399 (2017) 308–329, <https://doi.org/10.1016/j.jsv.2017.03.020>.
- [55] C. Liu, J. Teng, Kun Fang, Cluster-based optimal wireless sensor deployment for structural health monitoring, *Struct. Heal. Monit.* 17 (2) (2017), <https://doi.org/10.1177/1475921717689967b>.
- [56] M.Z.A. Bhuiyan, G. Wang, J. Wu, J. Cao, X. Liu, T. Wang, Dependable structural health monitoring using wireless sensor networks, *IEEE Trans. Dependable Secur. Comput* (2015), <https://doi.org/10.1109/TDSC.2015.2469655>.
- [57] S. Nagarajaiah, Y. Yang, Modeling and harnessing sparse and low-rank data structure: a new paradigm for structural dynamics, identification, damage detection, and health monitoring, *Struct. Control Heal. Monit.* (2017), <https://doi.org/10.1002/stc.1851>.
- [58] G. Hackmann, F. Sun, N. Castaneda, C. Lu, S. Dyke, A holistic approach to decentralized structural damage localization using wireless sensor networks, *Comput. Commun.* 36 (2012) 29–41, <https://doi.org/10.1016/j.comcom.2012.01.010>.
- [59] D.C. Ciresan, U. Meier, L.M. Gambardella, J. Schmidhuber, Deep, big, simple neural nets for handwritten digit recognition, *Neural Comput.* 22 (2010) 3207–3220, https://doi.org/10.1162/NECO_a_00052.
- [60] D. Scherer, A. Müller, S. Behnke, Evaluation of pooling operations in convolutional architectures for object recognition, in: *Proc. 20th Int. Conf. Artif. Neural Networks Part III*, Springer-Verlag, Berlin, Heidelberg, 2010, pp. 92–101, https://doi.org/10.1007/978-3-642-15825-4_10.
- [61] S. Kiranyaz, M.A. Waris, I. Ahmad, R. Hamila, M. Gabbouj, Face segmentation in thumbnail images by data-adaptive convolutional segmentation networks, in: *2016 IEEE Int. Conf. Image Process.*, 2016, pp. 2306–2310, <https://doi.org/10.1109/ICIP.2016.7532770>.
- [62] D.H. Hubel, T.N. Wiesel, Receptive fields of single neurones in the cat's striate cortex, *J. Physiol.* 148 (1959) 574–591.
- [63] S. Kiranyaz, T. Ince, M. Gabbouj, Personalized monitoring and advance warning system for cardiac arrhythmias, *Sci. Rep.* 7 (2017), <https://doi.org/10.1038/s41598-017-09544-z>.
- [64] S. Kiranyaz, T. Ince, M. Gabbouj, Real-time patient-specific ECG classification by 1-d convolutional neural networks, *IEEE Trans. Biomed. Eng.* 63 (2016) 664–675, <https://doi.org/10.1109/TBME.2015.2468589>.
- [65] T. Ince, S. Kiranyaz, L. Eren, M. Askar, M. Gabbouj, Real-time motor fault detection by 1-d convolutional neural networks, *IEEE Trans. Ind. Electron.* 63 (2016) 7067–7075, <https://doi.org/10.1109/TIE.2016.2582729>.
- [66] O. Janssens, V. Slavkovikj, B. Vervisch, K. Stockman, M. Locufier, S. Verstockt, R. Van de Walle, S. Van Hoecke, Convolutional neural network based fault detection for rotating machinery, *J. Sound Vib.* 377 (2016) 331–345, <https://doi.org/10.1016/j.jsv.2016.05.027>.
- [67] W. Zhang, C. Li, G. Peng, Y. Chen, Z. Zhang, A deep convolutional neural network with new training methods for bearing fault diagnosis under noisy environment and different working load, *Mech. Syst. Signal Process.* 100 (2018) 439–453, <https://doi.org/10.1016/j.ymssp.2017.06.022>.
- [68] L. Jing, T. Wang, M. Zhao, P. Wang, An adaptive multi-sensor data fusion method based on deep convolutional neural networks for fault diagnosis of planetary gearbox, *Sensors* 17 (2017) 414, <https://doi.org/10.3390/s17020414>.
- [69] O. Abdeljaber, A. Younis, O. Avci, N. Catbas, M. Gul, O. Celik, H. Zhang, Dynamic testing of a laboratory stadium structure, in: *Geotech. Struct. Eng. Congr.* 2016, 2016, pp. 1719–1728, <https://doi.org/10.1061/9780784479742.147>.
- [70] O. Abdeljaber, O. Avci, M.S. Kiranyaz, B. Boashash, H. Sodano, D.J. Inman, 1-D CNNs for structural damage detection: verification on a structural health monitoring benchmark data, *Neurocomputing* (2017), <https://doi.org/10.1016/j.neucom.2017.09.069>.
- [71] The Mathworks Inc, MATLAB - MathWorks, 2016 doi: 2016-11-26, www.mathworks.com/products/matlab.